Photoactive Antimicrobial PVA Hydrogel Prepared by Freeze-Thawing Process for Wound Dressing

Kyung Hwa Hong, Gang Sun

Division of Textiles and Clothing, University of California, Davis 95616, California

Received 9 September 2009; accepted 19 November 2009
DOI 10.1002/app.31827
Published online 14 January 2010 in Wiley InterScience (www.interscience.wiley.com).

ABSTRACT: A freeze-thawing process was employed to produce both rose bengal (RB)/polyvinyl alcohol (PVA) and benzophenone (BP)/PVA hydrogels, respectively. Results indicated that only RB incorporated PVA (RB/PVA) could form hydrogel after undergoing three cycles of freeze-thawing process; One of the cycles should be conducted by freezing at $-15°C \pm 3°C$ for 18 h followed by thawing at 25°C for 6 h. The structural features and functional properties of the RB/PVA hydrogel were investigated by FTIR, XRD, SEM evaluations, and photo-induced antimicrobial functions were examined as well. Release of RB from the RB/PVA hydrogel was examined by UV-Vis spectroscopy. The freeze-thawed RB/PVA hydrogel showed antimicrobial abilities against both *E. coli* and *S. aureus* under the exposure to fluorescence light as well as UVA (365 nm) light. © 2010 Wiley Periodicals, Inc. J Appl Polym Sci 116: 2418–2424, 2010

Key words: rose bengal; polyvinyl alcohol; photoactive antimicrobial agent; wound dressing

INTRODUCTION

Different wound dressings, such as wet and dry, are currently used for patients who have wounds caused by burns, split grafts, chronic ulcers, and decubitus ulcers.[1–4] However, it has been reported that wet environments promote faster healing than dry conditions.[5] As such, in recent years, hydrogels have received considerable attention because of their potential to be used as specific absorbents in wound dressing. Furthermore, a number of polymer materials with superabsorbent properties have been developed for clinical applications, such as liquefaction and removal of scars, treatment of leg ulcers, alleviation of sores, and prevention of tissue deterioration in patients with restricted mobility.[6,7]

Polyvinyl alcohol (PVA) has several useful properties, including nontoxicity, biocompatibility, high hydrophilicity, fiber/film-forming capabilities, and chemical and mechanical resistance. Because of these properties, PVA is now widely used in products such as temporary skin covers, cosmetics, pharmaceuticals, and burn dressings.[8,9] Additionally, insolubilized PVA hydrogels have more special applications. However, PVA has generally not been considered for use as a load bearing biomaterial, primarily because of its low modulus and poor wear characteristics.[10] Hydrogels are commonly known as hydrophilic three-dimensional networks held together by either chemical or physical bonds. Interstitial spaces existing within the network allow water molecules to become trapped and immobilized, filling the available free volume. Therefore, these hydrogels have been used to make artificial skin, contact lenses, interfaces between bones and implants, and matrices in drug delivery systems.[11] In particular, hydrogels from PVA aqueous solutions prepared by the freeze-thawing process have shown many interesting properties, including proper mechanical strength and stability at room temperature, and no involvement of any toxic initiator or cross-linker. Most importantly, however, these gels are nontoxic, noncarcinogenic, biocompable, and have desirable physical properties such as a rubbery nature and a high degree of swelling in water.[12]

In this study we prepared and investigated freeze-thawed PVA hydrogels incorporated with photoactive antimicrobial agents to produce functional composite materials with favorable mechanical performance and bio-friendly properties. Two photoactive antimicrobial agents, benzophenone (BP) and rose bengal (RB), were used in the formulations. BP is a good photosensitizer and has been used as a photoinitiator for reactions under ultraviolet radiation. Additionally, BP chromophoric groups were recently found to easily produce radicals under both UVA (365 nm) and fluorescent light irradiation.[13–15] RB is a xanthene photosensitizer with a high absorption coefficient in the visible region of the spectrum and a tendency to transfer electrons from its excited triplet state, producing long-lived radicals.[16,17]

Correspondence to: G. Sun (gysun@ucdavis.edu).
Contract grant sponsor: National Science Foundation; contract grant number: CTS-0424716.

EXPERIMENTAL

Materials

PVA (atactic, 87–89% hydrolyzed, average M_w 85,000–124,000) was purchased from Aldrich (Milwaukee, WI). BP (99% pure), RB (60% pure), and acetone were purchased from Acros Co. (NJ). All reagents were used as received without any further purification.

Preparation

PVA hydrogels were prepared by fully dissolving 10.0 g of polymer powder without further purification in 100 mL of distilled water, under magnetic stirring, at a temperature of 80°C ± 5°C. The 10% PVA (wt %) solution was cooled down to room temperature and 25 g of it were poured into each of three vials. Then, 1.5 g of BP/acetone solution (5 wt %) and 1.5 g of RB/water solution (5 wt %) were added into each of the vials containing 25 g of the PVA solution. The mixtures in vials were vigorous agitated. Subsequently, the vials, each of which containing pure PVA solution, BP/PVA solution, and RB/PVA solution, were frozen at −15°C ± 3°C for 18 h and thawed at 25°C for 6 h, for three consecutive cycles.

Each of the samples was then placed under different lamps for photoactivation. The lamps used were: five 8W (12″) ultra-violet (UV) lamp [BLE-8 T365 (bandwidth: ≈ 365 nm); sample to bulb distance: 15.8 cm, and five 8W (12″) fluorescent lamp (light output: 400 lm); sample to bulb distance: 15.8 cm].

Characterization

Fourier transform infrared (FTIR) spectroscopy was performed with a Nicolet 6700 FTIR spectrometer (Thermo Electron, Madison, WI) with a resolution of 4 cm^{-1}, and the measurements were carried out with an attenuated total reflectance (ATR) technique. UV-VIS absorption spectra were taken with an Evolution 600 UV-Visible spectrophotometer (Thermo Scientific, Waltham, MA) in a wavelength range of 200–800 nm with a 1-cm quartz cell. X-ray diffraction (XRD) measurements were performed at room temperature with Cu Kα X-rays (α = 1.5418 Å) with a D8 Advance (Bruker, Germany). A theta-theta wide angle goniometer was used, and the ultimate peak resolution was 2θ = 0.025°. The surface morphologies of hydrogels were examined using a scanning electron microscope (SEM; Philips XL30, Salem, MA). Thermogravimetric analysis (TGA) was carried out with a ShimadzuTGA-50apparatus (Shimadzu Scientific Instruments, Columbia, MD) at a heating rate of 10°C/min from 30 to 600°C under a nitrogen atmosphere. And differential scanning calorimetry (DSC), performed on a Shimadzu DSC-60 (Shimadzu) under nitrogen atmosphere with programmed heating of 10°C/min.

To obtain initial morphologies of the hydrogels, the samples were prepared by using the follow procedure: Immediately following the three cycles of freeze-thawing described in "Preparation" section, the hydrogels were immersed in 25°C distilled water, then rapidly frozen with liquid nitrogen, and dried in a vacuum at −50°C for 10 days. After the freeze-dry process, the samples were gold sputtered for 3 min to measure the swelling behaviors of the hydrogels. The hydrogels were subjected to the following process: first, the hydrogel samples were dried at 25°C in atmospheric conditions for 10 days, and their dry weights (W_d) were measured immediately. Then, the dried samples were soaked in 30°C distilled water for 2 days, and their weights (W_w) were measured again. The swelling ratio was calculated using the following formula (1):

$$\text{Swelling ratio } (\%) = \frac{W_w - W_d}{W_d} \times 100 \quad (1)$$

Antimicrobial properties of the hydrogels were evaluated against *Staphylococcus aureus* (*S. aureus*) (ATCC 12,600, a gram-positive bacterium) and *Escherichia coli* (*E. coli*) (K-12, a gram-negative bacterium), according to a modified testing method for antibacterial activity of films.[13–15] The diluted microbial aqueous solutions containing the hydrogels were illuminated under UVA light for 2 h. After a selected contact time, 0.1 mL of microbial suspension was taken from the container and then was diluted to 10^1, 10^2, 10^3, and 10^4 in series with distilled water. One hundred microliter of the dilution was placed onto agar plates and incubated at 37°C for 18 h. The same testing procedure was employed for a bacterial solution without hydrogel inside, serving as a control. The reduction of bacteria was calculated according to the following eq. (2):

$$\text{Reduction of bacteria } (\%) = \frac{(B - A)}{B} \times 100 \quad (2)$$

Where, A and B are the surviving cells (colony forming unit mL^{-1}) on the agar plates corresponding to the hydrogel sample and the control, respectively.

RESULTS AND DISCUSSION

Preparation and observation of freeze-thawed RB/PVA hydrogel

Only pure PVA solution and RB/PVA solution were successfully converted into gel state by the freeze-thawing process, as shown in Figure 1. BP/PVA solution did not form a gel structure because BP/

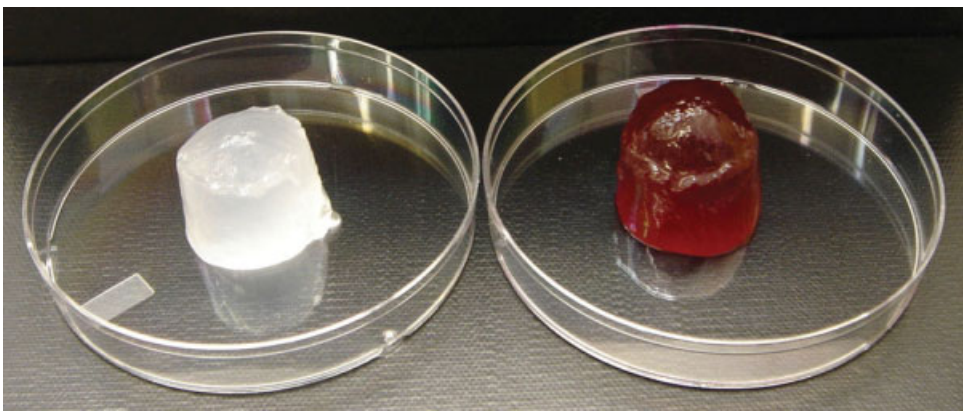

Figure 1 Surface morphologies of freeze-thawed PVA hydrogel (left) and freeze-thawed RB/PVA hydrogel (right). [Color figure can be viewed in the online issue, which is available at www.interscience.wiley.com.]

acetone solution dispersed in PVA aqueous solution prevented PVA from physical crosslinking. Therefore, here, only the freeze-thawed RB/PVA hydrogel was further investigated and discussed as the photoactivated functional dressing material. Figure 2 shows the surface morphologies of pure PVA film, freeze-thawed PVA hydrogel, and freeze-thawed RB/PVA hydrogel, respectively. Both PVA hydrogel and RB/PVA hydrogel definitely have a porous structure. And it was observed that fine particles evenly distributed on the surface of the RB/PVA hydrogel, possibly RB moieties. On the other hand, the swelling percentage of the PVA and RB/PVA hydrogels were 351.76 and 398.90%, respectively. These values are quite higher than those of PVA hydrogels that were chemically crosslinked by glutaraldehyde prepared in the previous study.[18]

Internal structures of freeze-thawed RB/PVA hydrogel

The physical gelation capability of the atactic and syndiotactic forms of PVA have been known for a long time,[19] when they are subjected to a series of freeze-thawing cycles. This is because upon the solvent frozen, crystals grow until they meet the facets of other crystals, and the effect of these crystals is the formation of a porous system upon thawing.[20] These physically crosslinked PVA gels, called cryogels, are reported to display various properties depending on the molecular weight of the polymer, the concentration of the aqueous PVA solution, the temperature and time of freezing and thawing, the number of freeze-thawing cycles, etc.[19] However, we observed that the crystalline C—O stretching vibration at 1142 cm^{-1} in the FTIR spectrum of PVA film, strongly depending on the degree and rate of crystallization of the PVA matrix,[21,22] decreased in the spectra of PVA hydrogel and RB/PVA hydrogel, as shown in Figure 3. This result indicates that the crystallinity of PVA reduced after forming the hydrogel by freeze-thawing process, and this trend is similar to that of chemically crosslinked PVA hydrogels.[22] Also, it was observed that the pattern of the stretching vibrations associated to alkane (2850–3000 cm^{-1}) of the PVA film and the PVA hydrogels prepared by the freeze-thawing process exhibited significant difference. Therefore, it seems that the PVA polymer chains have undergone a chemical crosslinking reaction during the freeze-thawing process rather than a physical process. This idea has a thread of connection with an earlier study,[23] which presented experimental results suggesting reconsideration of the origin of the gelation phenomenon in PVA during the freeze-thawing cycles. They found that the freeze-thawing procedure could simultaneously lead to breaking up PVA chains and increasing polymer molecular weight. In addition, growing water crystals in the gels during the freeze-thawing could induce a shearing effect within the polymer solution which may break up polymer chains and correspondingly create free radicals. And these free radicals are liable to react with other chains, leading to chemical crosslinks and high molecular weight material. This explanation reveals that the gelation through the freeze-thawing procedure was caused by chemical interactions, which was proven by the results of XRD and TGA analyzes. Figure 4 shows XRD patterns of PVA film, freeze-thawed PVA hydrogel, and freeze-thawed RB/PVA hydrogel, respectively. The PVA amorphous peak in the pattern of PVA film slightly shifted from 19.89 to 19.49 in the patterns of the freeze-thawed PVA hydrogel and RB/PVA hydrogel. Since $d \propto 1/\sin\theta$ (Bragg's law: $\lambda = 2d \sin\theta$), shifting left in the peak position indicates an increase in the lattice plane spacing of the hydrogel structures occurred during the freeze-thawing process.[24] The d-spacing increase in the hydrogels could be due to the fact that the breakage of PVA main

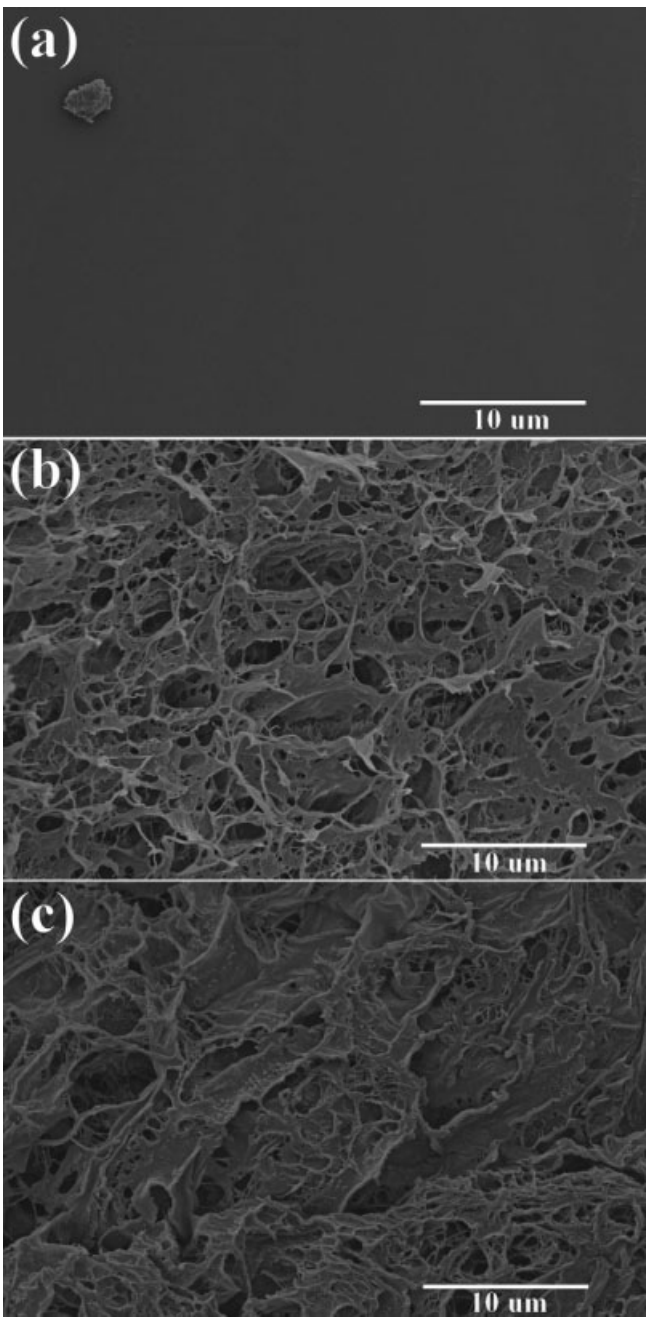

Figure 2 SEM images of the surface of PVA film (a), freeze-thawed PVA hydrogel (b), and freeze-thawed RB/PVA hydrogel (c); hydrogels are frozen dried before observation.

polymer chains lead to new crosslinkages and formation of a 3D networking structure of hydrogel during the freeze-thawing process. Figure 5 shows TGA curves of PVA film and the freeze-thawed PVA hydrogel. The amount of weight loss of the first stage on the curve increased from 6.5 to 13.9% after forming the hydrogel, indicating lower molecular weight portion and/or amorphous region in the PVA increased during the freeze-thawing process. The decomposition temperature of the freeze-thawed

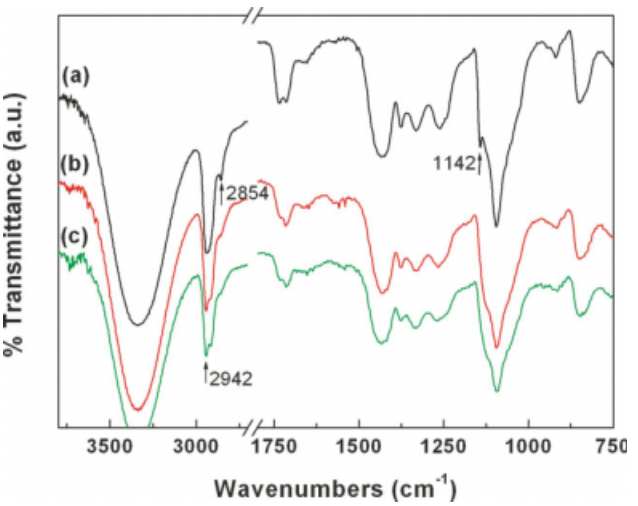

Figure 3 FTIR spectra of PVA film (a), freeze-thawed PVA hydrogel (b), and freeze-thawed RB/PVA hydrogel (c). [Color figure can be viewed in the online issue, which is available at www.interscience.wiley.com.]

PVA hydrogel (285°C) was slightly higher than that of PVA film (278°C), showing the crosslinked portion may increase in the hydrogel. On the other hand, no significant difference was observed in both FTIR and XRD spectra between the freeze-thawed PVA hydrogel and the freeze-thawed RB/PVA hydrogel. Thus, it was assumed that the amount of RB incorporated in PVA hydrogel (ca. 0.299 wt %) did not affect the formation of PVA hydrogel during the freeze-thawing process.

Figure 6 shows the DSC thermograms of PVA film, freeze-thawed PVA hydrogel, and freeze-thawed RB/PVA hydrogel, respectively. Melting endothermic peak (T_m) of PVA normally appears at around 228°C.[25] However it was observed that the

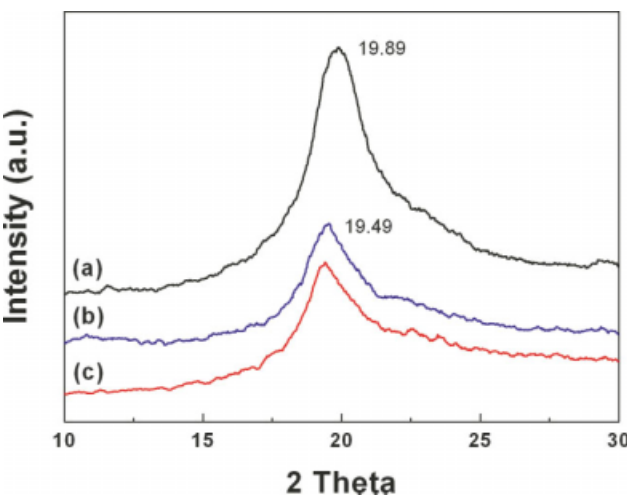

Figure 4 XRD patterns of PVA film (a), freeze-thawed PVA hydrogel (b), and freeze-thawed RB/PVA hydrogel (c). [Color figure can be viewed in the online issue, which is available at www.interscience.wiley.com.]

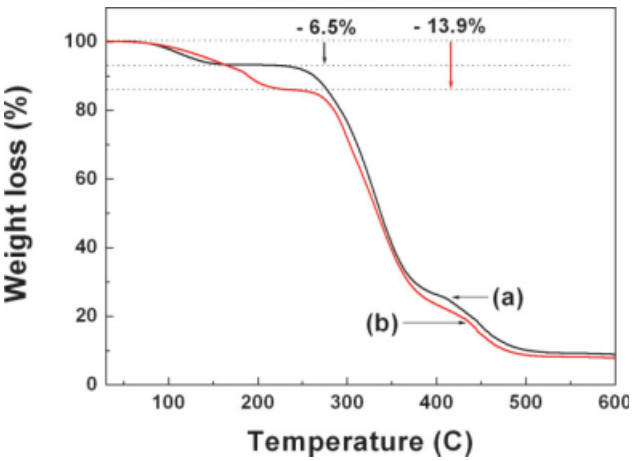

Figure 5 TGA curves of PVA film (a) and freeze-thawed PVA hydrogel (b). [Color figure can be viewed in the online issue, which is available at www.interscience.wiley.com.]

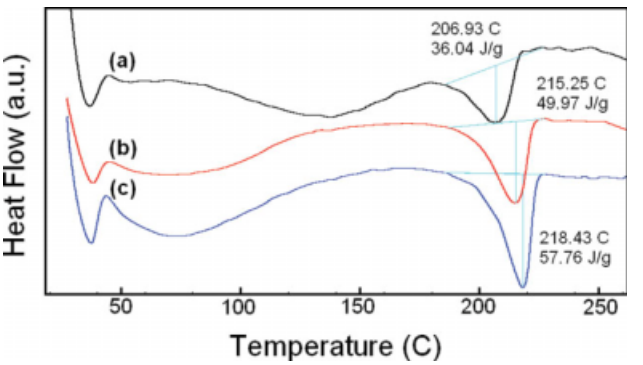

Figure 6 DSC thermograms of PVA film (a), freeze-thawed PVA hydrogel (b), and freeze-thawed RB/PVA hydrogel (c). [Color figure can be viewed in the online issue, which is available at www.interscience.wiley.com.]

peak showed up at around 210°C, and the enthalpy was 36.04 J/g for pure PVA film [Fig. 6(a)]. Different morphologies of PVA polymers could be developed by different crystallization processes. On the basis of the Heat of Fusion Rule of Burger and Ramberger,[26] more stable hydrogel should have higher enthalpy of fusion. Thus, the hydrogels appear to be monotropically related under normal pressure. Therefore, we believe that PVA polymer structure has gone through an irreversible transition formed from a metastable form (unstable form) to a stable structure during the freeze-thawing process.

Photo-activated antimicrobial ability

Photo-activated antimicrobial functions of the freeze-thawed RB/PVA hydrogel under different light sources were evaluated against *S. aureus* and *E. coli*, shown in Table I. It was known that the UVA light with 365 nm wavelength could not affect microbial growth.[13–15] The freeze-thawed RB/PVA hydrogel showed certain photo-induced antimicrobial activities against both *S. aureus* and *E. coli* under both UVA and fluorescent lights. RB is well known to effectively generate singlet oxygen ($^1O_2$, Reactive oxygen species) under UV light.[27] The singlet oxygen generated from the RB/PVA hydrogel under UVA light could be biocidal in the RB/PVA system, or it could produce H_2O_2 in existence of oxygen as proposed in Scheme 1, which is another biocide.[28–30]

RB release behavior of freeze-thawed RB/PVA hydrogel

Since RB was only blended into PVA system, the release of RB into water could occur, which may affect antimicrobial properties of the system. To

TABLE I
Antimicrobial Abilities of Freeze-Thawed RB/PVA Hydrogel Against *E. coli* and *S. aureus*. (Photo-Exposure to All of the Following Samples for 2 Hours)

		Dilution ratio of bacteria solution after contact time				Reduction of bacteria (%)
		10	10^2	10^3	10^4	
E. coli						
Under UVA light	Blank	∞	∞	121	16	–
	PVA hydrogel	∞	∞	37	1	69.42
	RB/PVA hydrogel	3	1	0	0	>99.92
Under fluorescent light	Blank	∞	∞	167	21	–
	PVA hydrogel	∞	∞	64	3	61.68
	RB/PVA hydrogel	8	5	1	0	>99.40
S. aureus						
Under UVA light	Blank	∞	∞	110	4	–
	PVA hydrogel	∞	134	36	0	67.28
	RB/PVA hydrogel	2	0	0	0	>99.85
Under fluorescent light	Blank	∞	∞	183	7	–
	PVA hydrogel	∞	∞	47	2	74.32
	RB/PVA hydrogel	3	0	0	0	>99.98

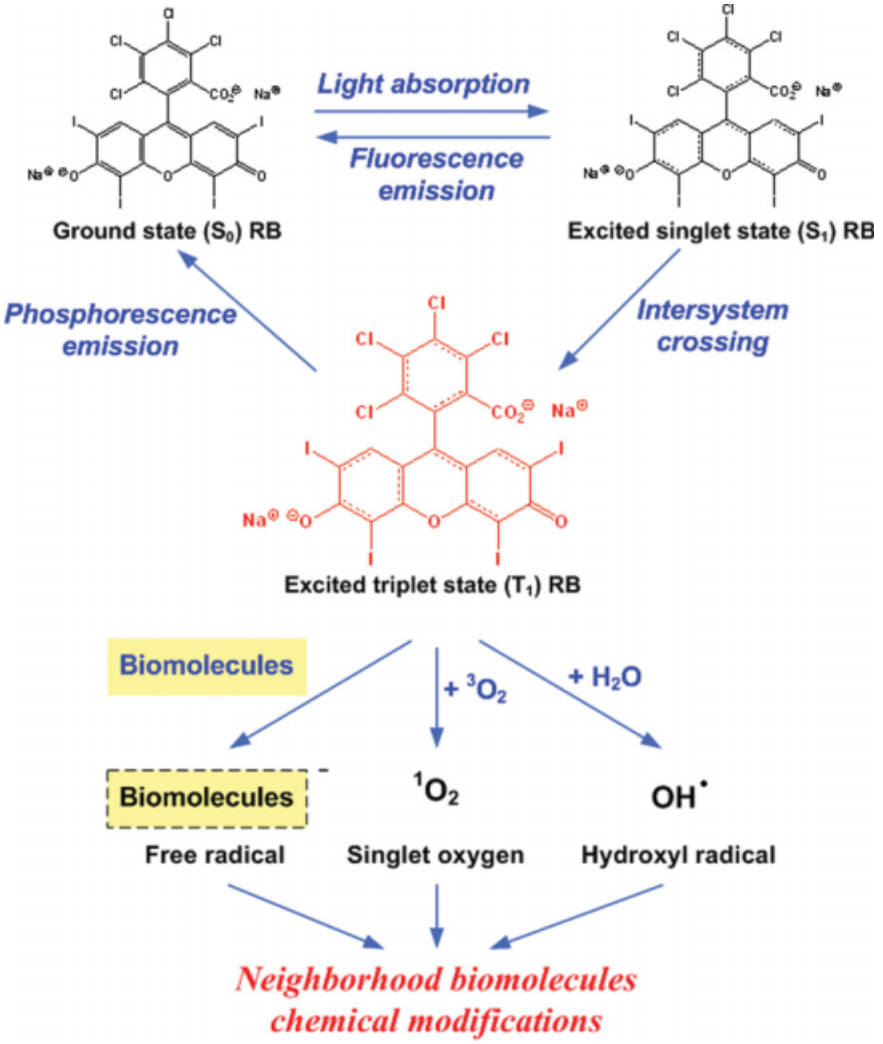

Scheme 1 Schematic diagram of reaction of RB/PVA hydrogel under photo-irradiation. [Color figure can be viewed in the online issue, which is available at www.interscience.wiley.com.]

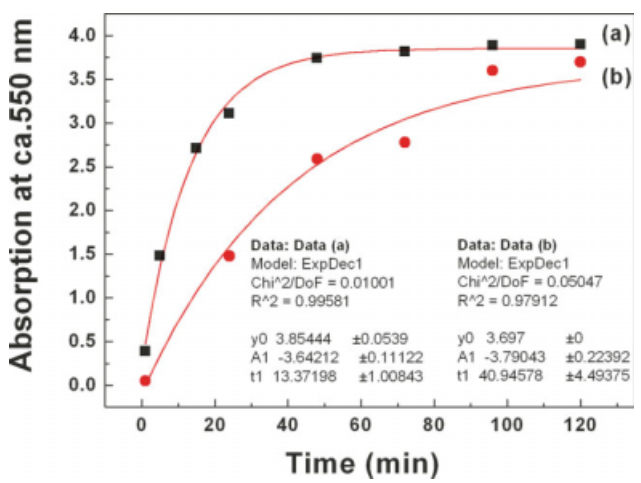

Figure 7 Absorption peak intensity at 550 nm of freeze-thawed RB/PVA hydrogel immersed water for first 120 h (a) and for second 120 h with new water (b). [Color figure can be viewed in the online issue, which is available at www.interscience.wiley.com.]

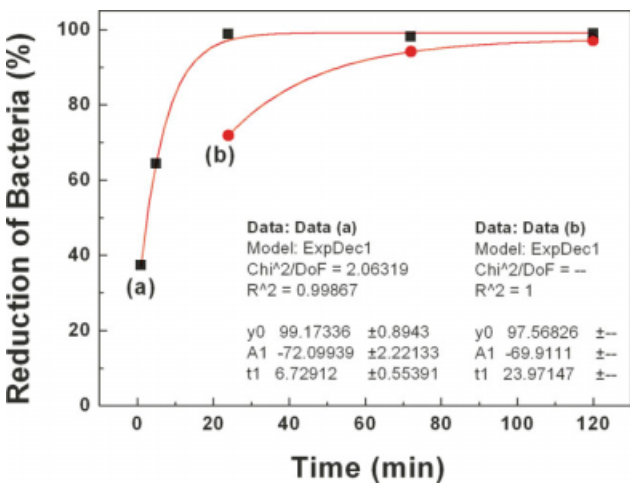

Figure 8 Antimicrobial abilities of freeze-thawed RB/PVA hydrogel immersed waters as a function of immersing time against *E. coli*. (UVA exposure to all of the following samples for 2 hours). [Color figure can be viewed in the online issue, which is available at www.interscience.wiley.com.]

investigate the RB release behavior of the freeze-thawed RB/PVA hydrogel, the hydrogel was immersed in 30°C ± 5°C distilled water for 120 h, and then the water samples were analyzed by a UV-Vis spectrometer at time intervals. Also, to study the durability of the RB release behavior of the RB/PVA hydrogels, the same measurement was repeated with the hydrogel after the first measurement. Through the analyzes, it was observed that initially the amount of RB moiety (λ_{Ab}= 550 nm) released from the freeze-thawed RB/PVA hydrogel increased with immersion time as shown in Figure 7(a). However, the release rate of RB reached equilibrium state at around 48 h after immersion. Furthermore, this release behavior repeatedly occurred when water was changed even though the concentration of released RB somewhat decreased as shown in Figure 7(b). Therefore, it was thought that the freeze-thawed RB/PVA hydrogel system could release the photoactive antimicrobial agent and control the concentration well under the wet scar condition. And, as expected, the RB/PVA water sample showed antimicrobial ability, as shown in Figure 8.

CONCLUSION

RB incorporated PVA hydrogel was successfully prepared by a process consisting of three cycles of freezing at −15°C ± 3°C for 18 h and followed by thawing at 25°C for 6 h. Through structural investigation of the hydrogels, it was assumed that PVA polymers became chemically crosslinked each other, and formed a hydrogel structure during the freezing-thawing process. And the freeze-thawed RB/PVA hydrogel showed excellent antimicrobial abilities under fluorescent light and UVA (365 nm) light, and the RB release behavior from the hydrogel to water was controlled by the environmental condition.

References

1. Dyson, M.; Young, S. R.; Pendle, L.; Webster, D. F.; Lang, S. J Invest Dermatol 1991, 91, 434.
2. Eaglstein, W. H.; Pittsburgh, M. D. J Am Acad Dermatol 1985, 12, 434.
3. Suzuki, Y.; Tanihara, M.; Nishmura, Y.; Suzuki, K.; Kakimura, Y.; Shimizu, Y. ASAIO J 1997, 43, 854.
4. Tanihara, M.; Suzuki, Y.; Nishimura, Y.; Suzuki, K.; Kakimaru, Y. Peptides 1998, 19, 421.
5. Winter, G. D. Nature 1962, 139, 293.
6. Kim, I. Y.; Yoo, M. K.; Seo, J. H.; Park, S. S.; Na, H. S.; Lee, H. C.; Kim, S. K.; Cho, C. S. Int J Pharm 2007, 341, 35.
7. Rujitanaroj, P.; Pimpha, N.; Supaphol, P. Polymer 2008, 49, 4723.
8. Peppas, N. A.; Scott, J. E. J Controlled Release 1992, 18, 95.
9. Yeo, J. H.; Lee, K. G.; Kim, H. C.; Oh, Y. L.; Kim, A. J.; Kim, S. Y. Biol Pharm Bull 2000, 23, 1220.
10. Muratoglu, O. K.; Spieqelberg, S. H.; Ruberti, J. W.; Abt, N. U.S. Pat. 20,060,079,597, 2006.
11. Juntanon, K.; Niamlang, S.; Rujiravanit, R.; Sirivat, A. Int J Pharm 2008, 356, 1.
12. Peppas, N. A.; Stauffer, S. R. J Controlled Release 1991, 16, 305.
13. Hong, K. H.; Sun, G. J Appl Polym Sci 2007, 106, 2661.
14. Hong, K. H.; Sun, G. Polym Eng Sci 2007, 47, 1750.
15. Hong, K. H.; Sun, G. Carbohydr Polym 2008, 71, 598.
16. Giulivi, C.; Sarcansky, M.; Rosenfeld, E.; Boveris, A. Photochem Photobiol 1990, 52, 745.
17. Kochevar, I. E.; Lambert, C. R.; Lynch, M. C.; Tedesco, A. C. Biochim Biophys Acta 1996, 1280, 223.
18. Hong, K. H.; Sun, G. Polym Sci Eng, to appear.
19. Hernández, R.; Sarafian, A.; López, D.; Mijangos, C. Polymer 2004, 45, 5543.
20. Mc Gann, M. J.; Higginbotham, C. L.; Geever, L. M.; Nugent, M. J. D. Pharm Nanotechnol 2009, 372, 154.
21. Lee, J. K.; Lee, J. L.; Jang, J. Polym Test 2008, 27, 360.
22. Mansur, H. S.; Sadahira, C. M.; Souza, A. N.; Mansur, A. A. P. Mater Sci Eng C 2008, 28, 539.
23. Hernandez, R.; Lopez, D.; Mijangos, C.; Guenet, J. Polymer 2002, 43, 5661.
24. Abdullah, M.; Panatarani, C.; Kim, T. O.; Okuyama, K. J Alloys Compd 2004, 377, 298.
25. Tubbs, R. K. J Polym Sci Part A: Gen Pap 1965, 3, 4181.
26. Burger, A.; Ramberger, R. Microchimica Acta 1975, 72, 1436.
27. Floyd, R. A. Free Radical Biol Med 2009, 46, 1004.
28. Abdullah, F. H.; Rauf, M. A.; Ashraf, S. S. Dyes Pigments 2005, 66, 129.
29. Hong, K. H.; Sun, G. J Appl Polym Sci 2010, 115, 1138.
30. Rauf, M. A.; Marzouki, N.; Körbahti, B. K. J Hazard Mater 2008, 159, 602.